IOSR Journal of Mechanical and Civil Engineering (IOSR-JMCE)
e-ISSN: 2278-1684,p-ISSN: 2320-334X, Volume 18, Issue 5 Ser. I (Sep. – Oct. 2021), PP 37-42
www.iosrjournals.org

Stress Analysis of Electrical Submersible Pump Shaft Using Computational Simulation: A preliminary Study

Yudianto[1], Agung Mataram[1], Akbar Teguh Prakoso[1], Diah Kusuma Pratiwi[1*]
[1]*Department of Mechanical Engineering, Faculty of Engineering, Universitas Sriwijaya, Kabupaten Ogan Ilir, Palembang, Sumatera Selatan, Indonesia.*
[*]*Corresponding author: pratiwi.diahkusuma@gmail.com*

Abstract
Shaft is a critical component in electrical submersible pump (ESP). In many cases, dismantle analyses are unable to identify a definitive root cause for shaft failure. Several hypotheses have been studied to explain shaft failure. In this paper, typical shaft failure modes will be reviewed, more specifically, the power source and the consequence of shaft failure will be discussed. Stress analysis of the premature failure of shaft used in electrical submersible pump (ESP) for lifting oil has been carry out using computational simulation. The results show, the maximum calculated Von Mises stress under torque 237 and 317 Nm were 402.51 MPa and 538.38 MPa respectively, and it were far below the yield strength of material. It may be concluded the premature failure of shaft not associated with high torsional load. It means the replacement of the motor from 120HP to 160 HP not influence to the fracture on ESP shaft. Need for further investigation of chemical material composition and mechanical properties of ESP shaft in order to obtain the root cause failure.

Keywords: *Electrical Submersible Pump, Finite Element Analysis, Shaft, Premature Failure*

Date of Submission: 27-08-2021 Date of Acceptance: 11-09-2021

I. Introduction

An electric submersible pump (ESP) is an artificial lift technique commonly used for oil and gas recovery from downhole reservoirs. It consists of multi-stage rotating impeller blades driven by medium voltage electric submersible AC motors. The pump-motor assembly in an ESP system is placed inside a downhole well, located hundreds to several thousands of meters below the surface. The pump blades while spinning increases the pressure of the reservoir fluid and forces it to reach the surface. The rate of oil recovery depends on the pressure produced by the ESP and is adjustable by varying the speed of the motor. Thus, ESPs can achieve a wide rate of production ranging from 200 to over 20,000 barrels of fluids per day [1]. Since the inception of ESPs, three-phase squirrel-cage induction submersible motors have been the de-facto technology as the prime mover. On the surface, the power supply to the submersible motor can be either a switchboard or a variable frequency drive (VFD) through a lengthy downhole cable. An ESP motor start-up directly from a switchboard supply creates a large starting current, which can be 6 to 9 times of the motor rated current, and thus introduces severe mechanical stress in the system [2][3][4][5]. This may expose the ESP shafts and interconnections to overload conditions and result in ESP failures [6][7][8]. Extended exposure to a fluctuating mechanical stress can also introduce fatigue in the system. Another investigation the reason of the pump shaft breakage is the bad pump assembly or the pump aging.

This study describes the failure analysis of a premature fracture ESP shaft that led to catastrophic consequences in terms of damage to other equipment and loss of production. Failure can also be less than catastrophic if detected early enough. It may mean a state of defectiveness, a lapse in manufacturing quality control or inspection effectiveness, the use of incorrect or below specification material, unexpected in-service deterioration, or damage through poor operation or maintenance. Even in these cases, the financial consequences can be high in terms of rework, repair, or remediation. The primary objective of a material's stress analysis is to determine the root cause of failure. Whether dealing with metallic or non-metallic materials, the root cause can normally be assigned to one of four categories; i.e., design, manufacturing, service or material. It also discussed the potential root causes of failure in the ESP shaft and the primary mode of failure. Included with the result of the failure analysis are recommendations for design improvements of the ESP system. If implemented, these recommendations should circumvent the possibility of failure of future ESP shaft system.

II. Material And Methods

The geographic location and the daily production of oil field as shown in figure 1. This well is "R" reservoir producer and can produce at least 1000 bbls/day. The failed component in the case study was a shaft from pump UT unit. Typical configuration of ESP system as shown figure 2. From the information of engineering staff, the failed shaft was made of Monel K500 and was only in services for below 1 week before experience these failures, which raised loss of production at the oil company.

Figure 1. Case study location Map

A though background investigation was conducted to identify possible contributing factors of failure. Several important facts were uncovered during this process that will be highlighted in detail in the following sections. The ESP is new installation and using motor 120 HP/1295V/59 A. The ESP has been successfully running in frequency of 50 Hz for four days. After four days working condition, the ESP undergo unplanned shutdown. The ESP failed to starting-up under normal and reverse condition. Then the ESP starting-up directly from a switchboard (60Hz) and consequently the cable and electric motor short. Service rig was conducted by replacing the cable and electric motor (160HP/2185V/46 A). The ESP was back to normal running condition with a frequency of 50Hz. After 2 days working condition the ESP returned to unplanned shutdown. The ESP was failed to starting-up under normal and reverse condition. The ESP starting-up again directly from a switchboard (60Hz) and finally shaft broken.

The primary objective of this investigation was to evaluate the stress on ESP shaft. In order to understand the problem, a detailed background study was performed. This stage of the investigation was the examination of the damaged parts and failure surfaces (see Fig 2). The fracture morphology observation of the shaft part removed from ESP component can be shown in figure 3. The curved concentric lines (beach marks) which indicate fatigue phenomenon during work cycle around the fracture surface was not found. Adjacent to the fracture surface, the shaft was fully twisted (red arrow) and the fracture is perpendicular to the axis of the shaft. It may be concluded the morphology of fracture is associated to ductile failure (red arrow). Additionally, a similar morphology was observed by previous study [9] and associated with torsional overload fracture.

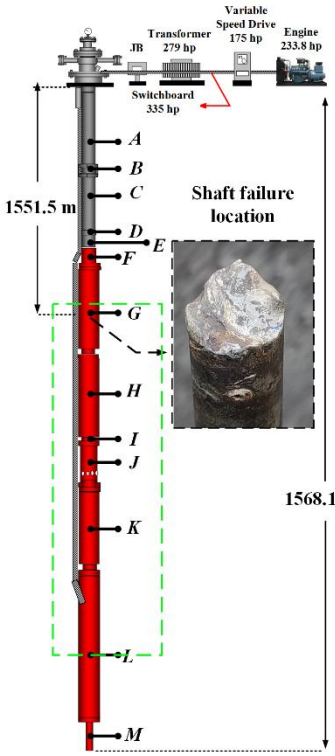

Abbrev	Item	Length (m)
A	Tubing	1520.099
B	Bleeder valve	0.149
C	1st joint tubing	9.501
D	Check valve	0.149
E	2nd joint tubing	19.001
F	BOH (Bolt on head)	0.152
G	Pump UT	3.194
H	Pump LT	3.650
I	Adaptor	0.100
J	Intake gas separator	1.080
K	Protector	2.740
L	Motor	7.673
M	ESP Centralizer	0.701

Figure 2. A typical configuration of an ESP System

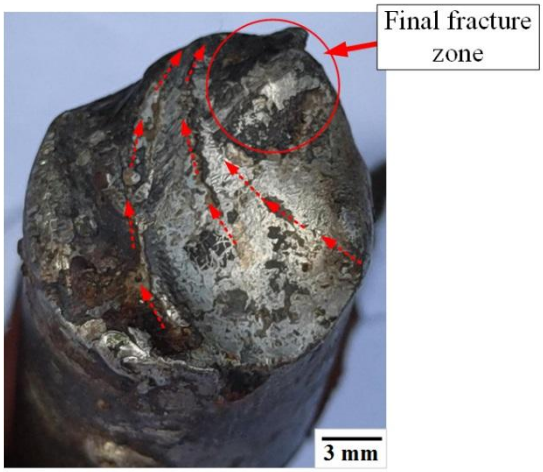

Figure 3. Evidence of failure was recovered from ESP shaft at 1550 meters from the ground level. The fracture zone is a typical brittle and ductile fracture.

In this study, the stress analysis using finite element approach. The finite element (FE) analysis was applied to analyze the stress distribution in the surroundings of ESP shaft and its relation to the fracture phenomenon. This study was performed to evaluate the effect of torsion load due to electric motor on the stress distribution on shaft. The geometry and FE analysis of ESP shaft were conducted using Solidworks software. The diameter of shaft is about 17,40mm. The boundary condition of this analysis as shown in Figure 4a. Torsion moment due to transmitted power from motor to the ESP shaft are about 237 Nm and 317 Nm respectively. The mesh of shaft was generated using a tetrahedral element with linear approximation (figure 4b). The material of shaft was assumed linear elastic material. The mechanical properties of Monel K-500 cold drawn-aged process for simulation purposes include E = 160 GPa, $\vartheta = 0.32$, $\sigma_y = 1103$ MPa, $\sigma_{ut} = 1276$ MPa [10].

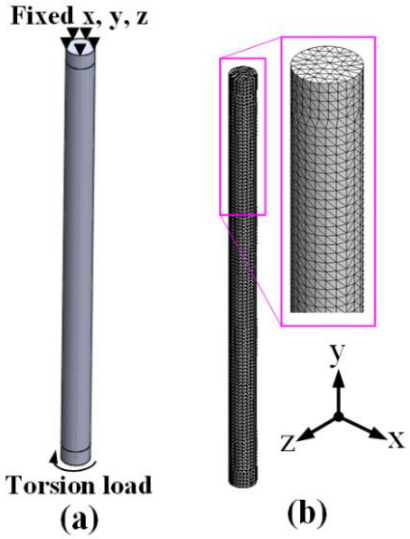

Figure. 4 a) Geometry of finite element model, b) Mesh setting

A mesh convergence study was conducted by running preliminary stress simulation on ESP shaft under torsion of 317 Nm. A mesh independence study aims to determine the optimum number of elements that will be used later in numerical calculations. The model is meshed with several element sizes (i.e. 833, 1716, 2526, 4573, 5079, 11148, 23017, 41146, 47006, and 50593). The result of the mesh refinement study is illustrated in Figure 5. The boundary conditions described above are used, and the Von Mises stress is calculated and plotted. The figure shows that 47006 elements a satisfactory numerical convergence with a margin of error of < 2% when the Von Mises stress is compared to the model with the smallest element size (i.e. 50593). By using the results in this mesh refinement study, the element size of 50k is represent to subjected all simulation of ESP shaft.

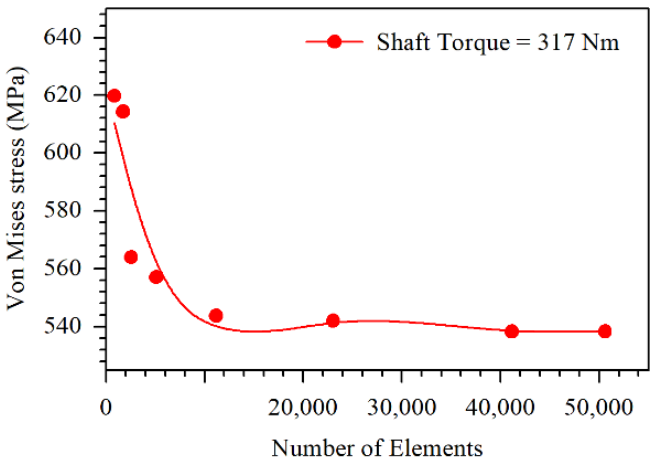

Figure 5. Mesh sensitivity study

III. Results And Discussion

The stress results from simulation as tabulated in Table1. The maximum calculated Von Mises stress under torque 237 and 317 Nm were 402.51 MPa and 538.38 MPa respectively, and it were far below the yield strength of material. Safety factor of shaft material above 1.5 which typical safety factor would be at least 1.5 – 4 [11]. From the result, the premature failure of ESP shaft was not caused by high torque load because the safety factor of shaft above 1.5. In addition, the visualization of Von Mises stress and shear stress of ESP shaft under difference torsion load as shown in Figure 6 and Figure 7 respectively.

Table 1. Simulation results

Power (HP)	Torsion load (Nm)	Results			
		Analytic	Simulation		
		Shear Stress (MPa)	Shear Stress (MPa)	Von mises stress (MPa)	Safety Factor
120	237	229.24	230.53	402.51	2.74
160	317	306.62	308.35	538.38	2.04

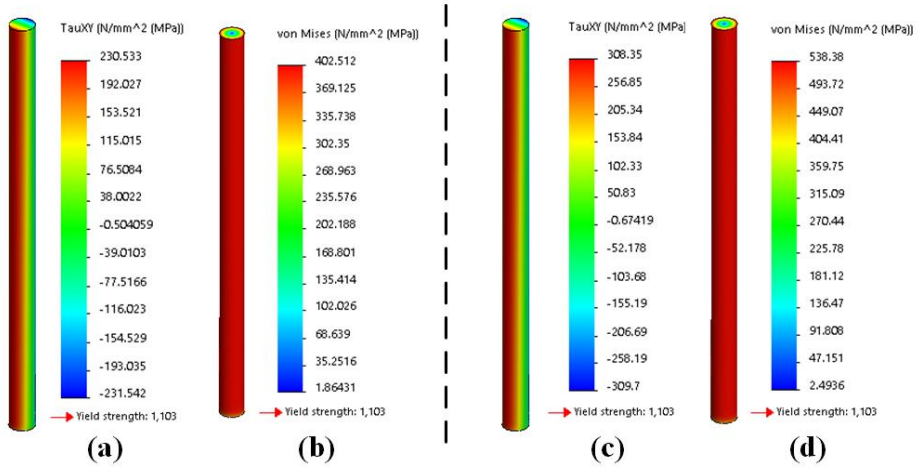

Figure 6. Stress analysis in ESP shaft; a) shear stress under torque load of 237 Nm, b) von mises stress under torque load of 237 Nm, c) shear stress under torque load of 317 Nm, d) von mises stress torque load of 317 Nm.

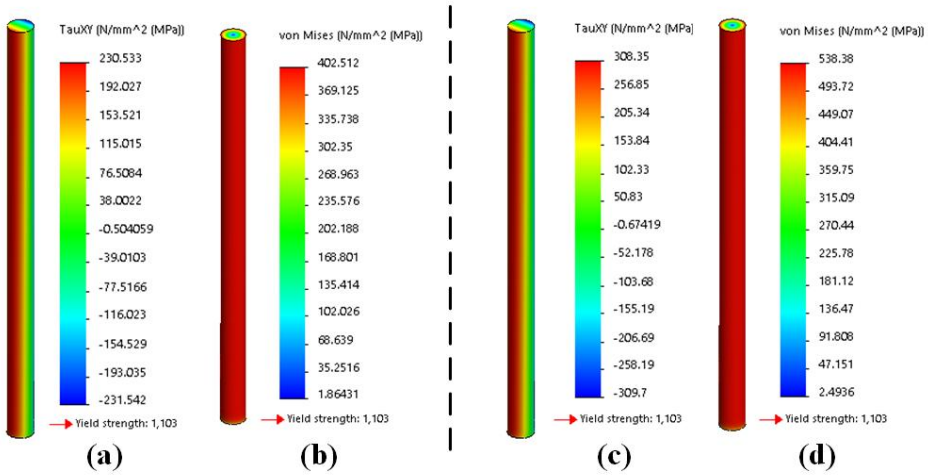

Figure 7. Stress analysis in ESP shaft; a) shear stress under torque load of 237 Nm, b) von mises stress under torque load of 237 Nm, c) shear stress under torque load of 317 Nm, d) von mises stress torque load of 317 Nm.

IV. Conclusion

The maximum Von Mises stress of ESP shaft under torque 237 and 317 Nm were 402.51 MPa and 538.38 MPa respectively, and it were far below the yield strength of Monel K500. Safety factor of shaft material above 1.5 which typical safety factor would be at least 1.5 – 4. It may be concluded the premature failure of shaft not associated with high torsional load. It means the replacement of the motor from 120 HP to 160 HP not influence to the fracture on ESP shaft. Need for further investigation of chemical material composition and mechanical properties of ESP shaft in order to obtain the root cause failure.

References

[1] O. Joel Romero and A. Hupp, "Subsea Electrical Submersible Pump Significance in Petroleum Offshore Production," *J. Energy Resour. Technol.*, 2014.

[2] R. A. Durham and T. R. Brinner, "Oilfield Electric Power Distribution," *IEEE Trans. Ind. Appl.*, 2015.

[3] O. V. Thorsen and M. Dalva, "Combined electrical and mechanical model of electric submersible pumps," *IEEE Trans. Ind. Appl.*, 2001.

[4] A. H. Vandermeulen, T. J. Natali, T. J. Dionise, G. Paradiso, and K. Ameele, "Exploring New and Conventional Starting Methods of Large Medium-Voltage Induction Motors on Limited kVA Sources," in *IEEE Transactions on Industry Applications*, 2019.

[5] K. Ledoux, P. W. Visser, J. D. Hulin, and H. Nguyen, "Starting large synchronous motors in weak power systems," *IEEE Trans. Ind. Appl.*, 2015.
[6] R. Pragale and D. D. Shipp, "Investigation of Premature ESP Failures and Oil Field Harmonic Analysis," *IEEE Trans. Ind. Appl.*, 2017.
[7] M. Farbis, A. H. Hoevenaars, and J. L. Greenwald, "Oil field retrofit of ESPs to meet harmonic compliance," *IEEE Trans. Ind. Appl.*, 2016.
[8] R. El-Mahayni, K. Al-Qahtani, and A. H. Al-Gheeth, "Large Synchronous Motor Failure Investigation: Measurements, Analysis, and Lessons Learned," *IEEE Trans. Ind. Appl.*, 2016.
[9] H. Sunandrio and . S., "ANALISIS KEGAGALAN SHAFT POMPA SUBMERSIBLE PADA UNIT PENGEBORAN MINYAK BUMI = FAILURE ANALYSIS OF PUMP SHAFT SUBMERSIBLE ON OIL DRILLING UNIT," *Mater. Kompon. dan Konstr.*, 2014.
[10] Special Metals Corporation, "High-Performance Alloys for Resistance to Aqueous Corrosion," 2000.
[11] R. G. Budynas and J. K. Nisbett, *Shigley's Mechanical Engineering Design, 9th Edition-McGraw-Hill*. 2017.

Yudianto, et. al. "Stress Analysis of Electrical Submersible Pump Shaft Using Computational Simulation: A preliminary Study." *IOSR Journal of Mechanical and Civil Engineering (IOSR-JMCE)*, 18(5), 2021, pp. 37-42.